III.4.3 The Future CERN Circular hadron collider

Massimo Giovannozzi
CERN, Geneva, Switzerland

The discovery of the Higgs boson, announced more than ten years ago (on 4th of July 2012), brought to completion the search for the fundamental constituents of matter and interactions that represent the so-called *Standard Model* (SM). Several experimental observations require an extension of the Standard Model. For instance, explanations are needed for the observed abundance of matter over antimatter, the striking evidence for dark matter, and the non-zero neutrino masses. Therefore, a new research infrastructure, based on a hadron collider of the highest energy, FCC-hh, with a center-of-mass collision energy of $100\,\mathrm{TeV}$ and an integrated luminosity of at least a factor of five greater than HL-LHC [1, 2] is proposed to address the aforementioned aspects [3–5]. This unique particle collider infrastructure, FCC-hh, will serve the world's physics community for about 25 years. However, it should be stressed that in combination with the lepton collider [6] as an initial stage, the integrated FCC project will provide a research tool until the end of the 21st century. The FCC construction project will be carried out in close collaboration with national institutes, laboratories and universities around the world, with the strong participation of industrial partners. It is worth mentioning that the coordinated preparatory effort is based on a core of an ever-growing consortium of more than 145 institutes worldwide.

III.4.3.1 Accelerator layout

The FCC-hh [3–5] is designed to provide proton–proton collisions with a center-of-mass energy of $100\,\mathrm{TeV}$ and an integrated luminosity of $\approx 20\,\mathrm{ab}^{-1}$ in each of the two primary experiments for 25 years of operation. The FCC-hh offers a very broad palette of collision types, as it is envisaged to collide ions with protons and ions with ions. The ring design also allows one interaction point to be upgraded to electron–proton and electron–ion collisions. In this case, an additional recirculating, energy-recovery linac will provide the electron beam that collides with one circulating proton or ion beam. The other experiments can operate concurrently with hadron collisions.

The FCC-hh will use the existing CERN accelerator complex as the injector facility. The accelerator chain, consisting of the CERN Linac4, PS, PSB, SPS, and LHC, could deliver beams at $3.3\,\mathrm{TeV}$ to FCC-hh, thanks to transfer lines using $7\,\mathrm{T}$ superconducting magnets that connect the LHC to FCC-hh. This choice also allows the continuation of CERN's rich and diverse fixed-target physics programme in parallel with FCC-hh operations. Limited modifications of the LHC should be implemented; in particular, the ramp speed can be increased to optimize the filling time of the FCC-hh.

The key parameters of the collider presented in the CDR are given in Table III.4.1. In the CDR, the circumference of FCC-hh was $97.75\,\mathrm{km}$. Recently, placement optimization has led to a "lowest-risk" layout with a circumference of $91.17\,\mathrm{km}$ (also see Section III.4.7 and Fig. III.4.1), comprising four short straight sections of $1.4\,\mathrm{km}$ length for experimental insertions, and four longer straight sections of about

This section should be cited as: The Future CERN Circular hadron collider, M. Giovannozzi, DOI: 10.23730/CYRSP-2024-003.1971, in: Proceedings of the Joint Universities Accelerator School (JUAS): Courses and exercises, E. Métral (ed.), CERN Yellow Reports: School Proceedings, CERN-2024-003, DOI: 10.23730/CYRSP-2024-003, p. 1971.

2.16 km each, that would house, e.g. the radiofrequency (RF), collimation, and beam extraction systems.

Two high-luminosity experiments are located in the opposite PA and PG insertions, which ensures the highest luminosity, reduces unwanted beam-beam effects, and is independent of the beam-filling pattern. The main experiments are located in 66 m long experimental caverns. Two additional, lower luminosity experiments are located in the other two experimental insertions.

Table III.4.1: Key FCC-hh baseline parameters from the 2019 CDR [3] compared to LHC and HL-LHC.

	LHC	**HL-LHC**	**FCC-hh**	
			Initial	**Nominal**
Physics performance and beam parameters				
Peak luminosity[1] (10^{34} cm^{-2}s^{-1})	1.0	5.0	5.0	< 30.0
Optimum average integrated luminosity/day (fb^{-1})	0.47	2.8	2.2	8
Assumed turnaround time (h)			5	4
Target turnaround time (h)			2	2
Peak number of inelastic events/crossing	27	135[2]	171	1026
Total/inelastic cross section σ proton (mb)	111/85		153/108	
Luminous region RMS length (cm)			5.7	
Distance IP to first quadrupole L^* (m)	23		40	
Beam parameters				
Number of bunches n	2808		10400	
Bunch spacing (ns)	25		25	
Bunch population N (10^{11})	1.15	2.2	1.0	
Nominal transverse normalized emittance (µm)	3.75	2.5	2.2	
Number of IPs contributing to ΔQ	3	2	$2+2$	2
Maximum total beam-beam tune shift ΔQ	0.01	0.015	0.011	0.03
Beam current (A)	0.58	1.12	0.5	
RMS bunch length[3] (cm)	7.55		8	
β^* (m)	0.55	0.15	1.1	0.3
RMS IP spot size (µm)	16.7	7.1	6.8	3.5
Full crossing angle (µrad)	285	590	104	200[4]

The regular lattice in the arc consists of 90° FODO cells with a length of about 213 m, six 14 m-long dipoles between the quadrupoles, and a dipole filling factor of about 0.8. Therefore, a dipole field around 16 T is required to maintain the nominal beams in the circular orbit.

The dipoles are based on Nb_3Sn and operated at 2 K. Increasing the current density in the conductors to 1500 A/mm^2 at 4.2 K, was successful [7, 8], and several optimized dipole designs have been developed within the framework of the EuroCirCol H2020 EC-funded project. Note that a US DOE

[1] For the nominal parameters, the peak luminosity is reached during the run.
[2] The baseline assumes leveled luminosity.
[3] The HL-LHC assumes a different longitudinal distribution; the equivalent Gaussian RMS is 9 cm.
[4] The luminosity reduction due to the crossing angle will be compensated using the crab crossing scheme.

Magnet Development Programme is actively working to demonstrate a $15\,\mathrm{T}$ superconducting accelerator magnet and has reached $14.5\,\mathrm{T}$. As the current plans are that FCC-hh is implemented following FCC-ee, the time scale for design and R&D for FCC-hh is of the order of 30 years. This additional time will be used to develop alternative technologies, such as magnets based on high-temperature superconductors with a potential significant impact on the collider parameters, relaxed infrastructure requirements (cryogenics system), and increased energy efficiency (temperature of magnets and beam screen).

III.4.3.2 Luminosity performance

The initial parameters, with a maximum luminosity of $5 \times 10^{34}\ \mathrm{cm^{-2}s^{-1}}$, are planned to be reached in the first years. Then a luminosity increase will be applied, to reach the nominal parameters with a luminosity of up to $3 \times 10^{35}\ \mathrm{cm^{-2}s^{-1}}$. Consequently, the integrated luminosity per day will increase from 2 to $8\,\mathrm{fb^{-1}}$. A luminosity of $2 \times 10^{34}\ \mathrm{cm^{-2}s^{-1}}$ can be achieved at the two additional experimental insertions, although further studies are needed to confirm this.

High-brightness and high-current beams, with a quality comparable to that of the beams of the HL-LHC, combined with a small β^* at the collision points ensure the high luminosity. The parasitic beam-beam interactions are controlled by introducing a finite crossing angle, whose induced luminosity reduction is compensated by means of crab cavities. Further improvement of machine performance might be achieved by using electron lenses and current-carrying wire compensators.

Fast burn-off under nominal conditions prevents the beams from being used for collisions for more than $3.5\,\mathrm{h}$. Hence, the turn-around time, i.e. the time from one luminosity run to the next one, is a critical parameter to achieve the target integrated luminosity. In theory, a time of about $2\,\mathrm{h}$ is within reach, but to include a sufficient margin, the turn-around times of $5\,\mathrm{h}$ and $4\,\mathrm{h}$ are assumed for initial and nominal parameters, respectively. Note that the availability of 70% at the flat top for physics operation is assumed for the estimate of the overall integrated luminosity.

III.4.3.3 Technical systems

Many technical systems and operational concepts for FCC-hh can be scaled up from HL-LHC or can be based on technology demonstrations carried out in the frame of ongoing R&D projects. Particular technological challenges arise from the higher total energy in the beam (20 times that of LHC), the much increased collision debris in the experiments (40 times that of HL-LHC), and far higher levels of synchrotron radiation in the arcs (200 times that of LHC).

High luminosity and beam energy will produce collision debris with a power of up to $0.5\,\mathrm{MW}$ in the main experiments, with a significant fraction of this lost in the ring close to the experiment. A sophisticated shielding system, similar to HL-LHC [2], protects the final focusing triplet, avoids quenches, and reduces the radiation dose. The current radiation limit of $30\,\mathrm{MGy}$ for magnets, imposed by the resin used, will be reached for an integrated luminosity of $13\,\mathrm{ab^{-1}}$, but an improvement is projected to be possible for both shielding and radiation hardness of magnets.

The robust collimation and beam extraction system protects the machine from the energy stored in the beam. However, the design of the collimation system is based on the LHC system [2,9], with several improvements.

The extraction system uses a segmented, dual-plane dilution kicker system to distribute the bunches in a multi-branch spiral on the absorber block. Novel superconducting septa capable of deflecting high-energy beams are currently being developed. Investigations of suitable absorber materials, including 3D carbon composites and carbon foams, are ongoing in the framework of the HL-LHC project.

The cryogenic system must compensate the continuous heat loads in the arcs of $1.4\,\mathrm{W/m}$ at a temperature below $2\,\mathrm{K}$, and the $30\,\mathrm{W/m/aperture}$ due to synchrotron radiation at a temperature of $50\,\mathrm{K}$, as well as absorbing the transient loads from the magnets ramping. The system must also be able to fill and cool the cold mass of the machine in less than 20 days, while avoiding thermal gradients higher than $50\,\mathrm{K}$ in the cryomagnet structure. Furthermore, it must also cope with quenches of the superconducting magnets and be capable of a fast recovery from such situations that leaves the operational availability of the collider at an adequate level.

The cryogenic beam vacuum system ensures excellent vacuum to limit beam-gas scattering and protect the magnets from the synchrotron radiation of the high-energy beam, also efficiently removing the heat. It also avoids beam instabilities due to parasitic beam-surface interactions and electron-cloud effects.

The beam screen features an anti-chamber and is copper coated to limit the parasitic interaction with the beam; the shape also reduces the seeding of the electron cloud by backscattered photons, and additional carbon coating or laser treatment prevents the build-up. This novel system is operated at $50\,\mathrm{K}$ and a prototype has been experimentally validated at the KARA synchrotron radiation facility at KIT (Germany).

The RF system is similar to that of the LHC with an RF frequency of $400\,\mathrm{MHz}$, although it provides a higher maximum total voltage of $48\,\mathrm{MV}$. The current design uses 24 single-cell cavities. To adjust the bunch length in the presence of longitudinal damping by synchrotron radiation, a controlled longitudinal emittance blow-up with band-limited RF phase noise is implemented.

III.4.3.4 Ion operation

A first set of parameters has been developed for the operation of ions on the basis of current injection performance. If two experiments operate simultaneously for 30 days, an integrated luminosity in each of them of $6\,\mathrm{pb}^{-1}$ and $18\,\mathrm{pb}^{-1}$ can be expected for proton-lead-ion operation with initial and nominal parameters, respectively. For lead-ion lead-ion operation $23\,\mathrm{nb}^{-1}$ and $65\,\mathrm{nb}^{-1}$ could be expected, although more detailed studies are being conducted to address the key issues in the production and collimation of ions and review luminosity predictions.

III.4.4 Civil engineering

As stated above, the FCC-hh collider will be installed in a quasicircular tunnel composed of arc segments interleaved with straight sections with an inner diameter of at least $5.5\,\mathrm{m}$ and a circumference of $91.17\,\mathrm{km}$. The internal diameter tunnel is required to house all the necessary equipment for the machine, while providing sufficient space for transport and ensuring compatibility between the FCC-hh and FCC-ee requirements. Figure III.4.1 shows the tunnel cross section in a typical arc region, including several ancillary systems and services required. Furthermore, about $8\,\mathrm{km}$ of bypass tunnels, about 18 shafts, 10 large caverns, and 8 new surface sites are part of the infrastructure to be built.

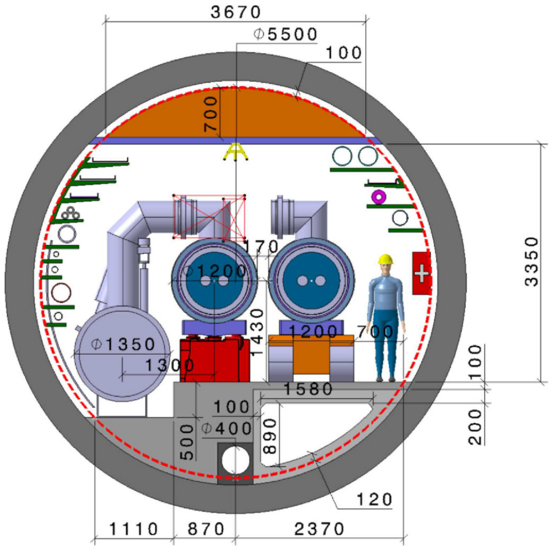

Fig. III.4.1: Cross section of the FCC-hh tunnel of an arc (from [3]). The gray equipment on the left represents the cryogenic distribution line. A 16 T superconducting magnet is shown in the middle, mounted on a red support element. An orange transport vehicle with another superconducting magnet is also shown in the transport passage.

The underground structures should be located as much as possible in the sedimentary rock of the Geneva basin, known as molasse (which provides good conditions for tunneling), and avoid the limestone of the nearby Jura. Furthermore, the depth of the tunnel and the shafts should be minimized to control the overburden pressure on the underground structures and to limit the length of the service infrastructure. These requirements, along with the constraint imposed by the connection to the existing accelerator chain through new beam transfer lines, led to a clear definition of the study boundary, which should be respected by all possible tunnel layouts considered. A slope of 0.2% in a single plane will be used for the tunnel to optimize the geology intersected by the tunnel and the depth of the shafts, as well as to implement a gravity drainage system. The majority of the machine tunnel will be constructed using tunnel boring machines, while the sector passing through limestone will be mined.

The CDR study was based on geological data from previous projects and data available from national services, and based on this knowledge, the civil engineering project is considered feasible, both in terms of technology and project risk control. Dedicated ground and site investigations are required during the early stage of the preparatory phase to confirm the findings, to provide a comprehensive technical basis for an optimized placement, and as preparation for project planning and implementation processes. For access points and their associated surface structures, the priority has been given to the identification of possible locations that are feasible from socio-urbanistic and environmental perspectives. Even in this case, the technical feasibility of the construction has been studied and is deemed achievable.

III.4.5 Detector considerations

The FCC-hh is both a discovery machine and a precision measurement machine, with the mass reach increased with respect to the current LHC by a factor of seven. The much larger cross sections for SM processes combined with the higher luminosity lead to a significant increase in measurement precision. This implies that the detector must be capable of measuring multi-TeV jets, leptons, and photons from heavy resonances with masses up to $50\,\mathrm{TeV}$, as well as the known SM processes, with high precision, and to be sensitive to a broad range of BSM signatures at moderate transverse momentum. Given the low mass of SM particles compared to the $100\,\mathrm{TeV}$ collision energy, many SM processes feature a significant forward boost while keeping transverse-momentum distributions comparable to LHC energies. Therefore, a detector for $100\,\mathrm{TeV}$ must increase the acceptance of precision tracking and calorimetry to $|\eta| \approx 4$, where $\eta = -\ln\left[\tan\left(\frac{\theta}{2}\right)\right]$, θ being the angle between the momentum of the particle and the direction of the beam, is called pseudorapidity, while retaining the transverse momentum thresholds for triggering and reconstruction at levels close to those of the current LHC detectors. The large number of p–p collisions per bunch crossing, leading to the so-called pile-up, imposes stringent criteria on the detector design. Indeed, the present LHC detectors cope with pile-up up to 60, the HL-LHC will generate values of up to 135, whereas the expected value of 1000 for the FCC-hh poses a technological challenge. Novel approaches, specifically in the context of high-precision timing detectors, will likely allow such numbers to be handled efficiently.

Figure III.4.1 shows the conceptual FCC-hh reference detector, which serves as a concrete example for subsystem and physics studies aimed at identifying areas where dedicated R&D efforts are needed. The detector has a diameter of $20\,\mathrm{m}$ and a length of $50\,\mathrm{m}$, similar to the dimensions of the ATLAS detector at the LHC. The central detector, with a coverage of $|\eta| < 2.5$, houses the tracking, electromagnetic calorimetry, and hadron calorimetry surrounded by a $4\,\mathrm{T}$ solenoid with a bore diameter of $10\,\mathrm{m}$. The required performance for $|\eta| > 2.5$ is achieved by moving the forward parts of the detector away from the interaction point, along the beam axis. Two forward magnet coils, generating a $4\,\mathrm{T}$ solenoid field, with an inner bore of $5\,\mathrm{m}$ provide the required bending power. Within the volume covered by the solenoids, high-precision momentum spectroscopy is ensured up to $|\eta| \approx 4$ and tracking up to $|\eta| \approx 6$. Alternative layouts are also studied for the magnets in the forward region [3].

In the reference detector, the magnetic field is unshielded, with several positive side effects that concur with a sensible cost reduction. The unshielded coil can be lowered through a shaft of $15\,\mathrm{m}$ diameter and the detector can be installed in a cavern of $37\,\mathrm{m}$ height and $35\,\mathrm{m}$ width, similar to the current ATLAS cavern. The magnetic stray field reaches $5\,\mathrm{mT}$ at a radial distance of $50\,\mathrm{m}$ from the beamline, so that no relevant stray field leaks in the service cavern, placed $50\,\mathrm{m}$ away from the experiment cavern and separated by rock. The shower and absorption processes inside the forward calorimeter produce a large number of low-energy neutrons, a significant fraction of which enters the tracker volume. To keep these neutrons from entering the muon system and the detector cavern, a heavy radiation shield is placed around the forward solenoid magnets to close the gap between the endcap and forward calorimeters.

III.4.6 Cost and schedule

In the FCC integrated project, FCC-hh is preceded by the Higgs, top, and electroweak factory, the lepton collider FCC-ee. Here, both the civil engineering and the general technical infrastructure of FCC-ee can be fully reused for FCC-hh, thus substantially lowering the investments for the latter to 17 BCHF, according to the CDR estimate [3]. The investments related to the particle collider and injectors amount to 80% of the cost of FCC-hh, that is, approximately 13.6 BCHF. The largest part of this accelerator cost corresponds to the expected price of the 4700 Nb_3Sn 16 T main dipole magnets, totaling 9.4 BCHF, for a target cost of 2 MCHF/magnet. For completeness, we note that in the CDR, the construction cost for FCC-hh as a single standalone project, i.e., without prior construction of an FCC-ee lepton collider, was estimated to be approximately 24 BCHF for the entire project.

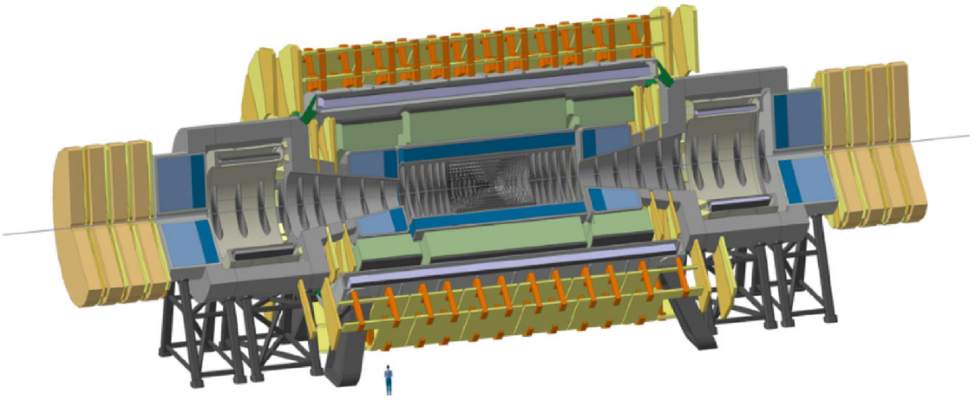

Fig. III.4.1: Conceptual layout of the FCC-hh reference detector (from [3]). It has an overall length of 50 m and a diameter of 20 m. A central solenoid with 10 m diameter bore and two forward solenoids with 5 m diameter bore provide a 4 T field for momentum spectroscopy throughout the tracking volume.

The FCC-hh operating costs, other than the electricity cost, are expected to remain limited, based on the evolution from LEP to LHC operation today, which shows a steady decrease in the effort needed to operate, maintain, and repair the equipment.

In the integrated FCC project, the disassembly of the FCC-ee and subsequent installation of the FCC-hh take about 8–10 years. The projected duration for the operation of the FCC-hh facility is 25 years, to complete the currently envisaged proton-proton collision physics programme. As a combined, "integrated" project, namely FCC-ee followed by FCC-hh, the FCC covers a total span of at least 70 years, i.e. until the end of the 21st century.

III.4.7 Progress since the CDR

Among the several domains of activity that have been pursued since the publication of the CDR, it is important to stress the intense efforts devoted to placement studies that refined the results of [3] with the goal of determining an optimal tunnel layout, in terms of geological situation, territorial, and environmental aspects. Furthermore, within the framework of FCC-ee studies, it emerged that implementing four experimental interaction points is an interesting option worth investigating. Beam dynamics considerations impose a symmetric positioning of the four experimental points. Hence, to allow sharing of the experimental caverns between the FCC-ee and its hadron companion, the same principle should also be applied to the FCC-hh lattice. The outcome of these considerations is the new layout shown in Fig. III.4.1. The circumference of the proposed layout is 91.17 km. The proposed layout has an appealing side effect, namely, only eight access points are present, with a non-negligible impact on the civil engineering works and costs.

The four experimental points are located in PA, PD, PG, and PJ, respectively. The length of the straight sections has been revised, following the results of the placement studies: a short straight section, $1.4\,\mathrm{km}$ in length like in the baseline lattice, is used to house the experimental interaction points; a long straight section, $2.16\,\mathrm{km}$ in length, is used to house the key systems. Currently, it is proposed to install the beam dump in PB, the betatron collimation in PF, the momentum collimation in PH, and the RF system in PL. These preliminary assignments should be confirmed by detailed studies. Such studies should also assess the feasibility of the optics required for the various systems, following the significant length reduction (from $2.8\,\mathrm{km}$ of the baseline CDR version to $2.16\,\mathrm{km}$ for the new version).

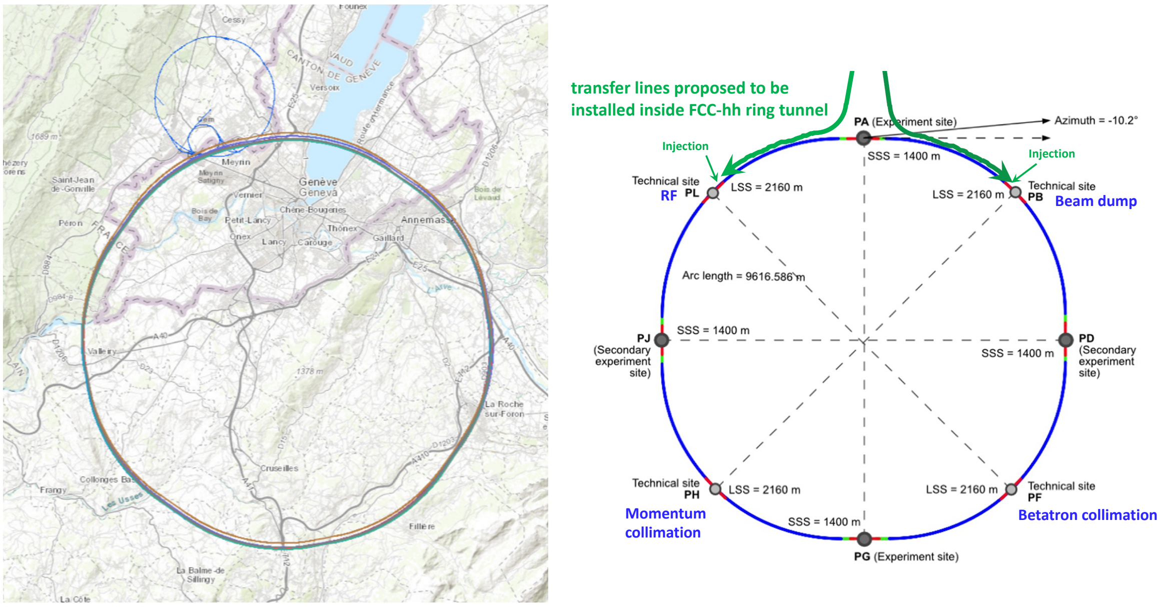

Fig. III.4.1: Left: Picture of some of the FCC implementation variants studied, including the LHC and SPS accelerators. Right: Sketch of the proposed superperiodic FCC-hh layout with eight surface sites.

The total length of the arcs is $76.93\,\mathrm{km}$, and, unlike the CDR configuration, all the arcs have the same length. The reduced total arc length implies that the collision energy falls short of $100\,\mathrm{TeV}$ by a few TeV, and this is not perceived as a hurdle. The FODO cell length is unchanged.

The rearrangement of the experimental points has an impact on the design of the injection and transfer lines. The current view consists of combining the injection with the beam dump (in PB) and with RF (in PL). Then, to save tunnel length, it is proposed that the transfer lines run in the FCC-hh ring tunnel from close to PA to the injection point (see Fig. III.4.1). An additional benefit of this solution is that the transfer line magnets in the ring tunnel would be normal-conducting. Integration of the transfer lines into the ring tunnel is actively being pursued to assess the feasibility of this proposal.

In parallel to studies for the optimization of the baseline layout, some efforts have been devoted to the analysis of alternative approaches to the generation of the ring optics. Indeed, the standard paradigm for collider optics consists in using separate-function magnets, in particular in the regular arcs, in conjunction with a FODO structure. However, a combined-function optics might provide interesting features, particularly appealing for an energy-frontier collider. A combined-function optics has the potential of providing a higher dipole filling factor, thus opening up interesting optimization paths of the dipole field and beam energy. Currently, this research has explored the benefits of a combined-function periodic cell [10]. It also optimized some of the cell parameters, such as its length [11], showing that the combined-function magnet is equally feasible as the baseline magnet. Furthermore, complex optics, including arc and dispersion suppressors, can indeed be realized with combined-function magnets. As a next step, the investigations will consider the various systems of corrector magnets planned in the baseline FODO cell and optimize them in the context of a combined-function periodic cell. Note that the latest developments of the design of the FCC-hh can be found in Refs. [12–14].

III.4.8 Conclusions

The FCC-hh baseline comprises a power-saving, low-temperature superconducting magnet system based on the evolution of the Nb_3Sn technology pioneered at the HL-LHC. An energy-efficient cryogenic refrigeration infrastructure and a high-reliability and low-loss cryogenic distribution infrastructure are also key elements of the baseline. Highly segmented kickers, superconducting septa and transfer lines, and local magnet energy recovery are other essential components of the proposed FCC-hh design. Furthermore, technologies that are already being gradually introduced at other CERN accelerators will be deployed in the FCC-hh. Given the time scale of the integrated FCC programme that allows for around 30 years of R&D for FCC-hh, an increase in the energy efficiency of a particle collider can be expected due to high-temperature superconductor R&D, carried out in close collaboration with industrial partners. Reuse of the entire CERN accelerator chain, which also serves a concurrent physics programme, is an essential lever to achieve a sustainable overall research infrastructure at the energy frontier.

The FCC-hh will be a strong motor of economic and societal development in all participating nations because of its large-scale and intrinsic character of the international fundamental research infrastructure, combined with the close participation of industrial partners. Finally, it is worth stressing the training provided at all levels of education by this marvelous scientific tool.

References

[1] O. Brüning and L. Rossi, The High-Luminosity Large Hadron Collider, *Nature Rev. Phys.* **1** (2019) 241, doi:10.1038/s42254-019-0050-6.

[2] I. Béjar Alonso *et al.*, High-Luminosity Large Hadron Collider (HL-LHC): Technical design report, CERN-2020-010 (CERN, Geneva, 2020), doi:10.23731/CYRM-2020-0010.

[3] A. Abada *et al.*, FCC-hh: The Hadron Collider: Future Circular Collider, conceptual design report, vol. 3, *Eur. Phys. J. Spec. Top.* **228** (2019) 755, doi:10.1140/epjst/e2019-900087-0.

[4] M. Benedikt and F. Zimmermann, The physics and technology of the Future Circular Collider, *Nature Rev. Phys.* **1** (2019) 238, doi:10.1038/s42254-019-0048-0.

[5] M. Benedikt *et al.*, Future Circular Colliders succeeding the LHC, *Nature Phys.* **16** (2020) 402, doi:10.1038/s41567-020-0856-2.

[6] A. Abada *et al.*, FCC-ee: The lepton collider, *Eur. Phys. J. Spec. Top.* **228** (2019) 261, doi:10.1140/epjst/e2019-900045-4.

[7] X. Xu *et al.*, Achievement of FCC specification in critical current density for N_3Sn superconductors with artificial pinning centers, arXiv:1903.08121 (2019), doi:10.48550/arXiv.1903.08121.

[8] S. Balachandran *et al.*, Beneficial influence of Hf and Zr additions to Nb4at%Ta on the vortex pinning of Nb_3Sn with and without an O source, *Supercond. Sci. Technol.* **32** (2019) 044006, doi:10.1088/1361-6668/aaff02.

[9] O.S. Brüning *et al.*, LHC design report: v.1, The LHC Main Ring, CERN-2004-003-V-1, (CERN, Geneva 2004), doi:10.5170/CERN-2004-003-V-1.

[10] M. Giovannozzi and E. Todesco, Combined-function optics for circular high-energy hadron colliders, *Eur. Phys. J. Plus* **137** (2022) 361, doi:10.1140/epjp/s13360-022-02583-0.

[11] M. Giovannozzi, Considerations on combined-function optics for high-energy storage rings and colliders, *EPJ Tech. Instrum.* **9** (2022) 5, doi:10.1140/epjti/s40485-022-00081-2.

[12] A. Abramov, R. Bruce, M. Giovannozzi, G. Perez-Segurana, S. Redaelli, and T. Risselada, “Collimation system for the updated FCC-hh design baseline”, presented at the IPAC’23, Venice, Italy, May 2023, paper MOPA127, doi:10.18429/JACoW-IPAC2023-MOPA127.

[13] E. Todesco and M. Giovannozzi, “Combined-function optics for the lattice of the CERN hadron-hadron Future Circular Collider ring”, presented at the IPAC’23, Venice, Italy, May 2023, paper MOPL032, doi:10.18429/JACoW-IPAC2023-MOPL032.

[14] M. Giovannozzi A. Abramov, W. Bartmann, M. Benedikt, R. Bruce, G. Perez-Segurana, T. Risselada, F. Zimmermann, “Recent updates of the layout of the lattice of the CERN hadron-hadron Future Circular Collider”, presented at the IPAC’23, Venice, Italy, May 2023, paper MOPL033, doi:10.18429/JACoW-IPAC2023-MOPL033.